Available online at www.sciencedirect.com

ScienceDirect

ARTICLE

Corrosion Behavior of W-Mo Co-Penetrated Layer Produced by Glow Discharge Plasma Technique in Acid Solution

Chen Fei[1],   Zhang Yulin[1],   Liu Weiguang[2],   Feng Wenran[1],   Yang Yingge[1]

[1] Beijing Key Laboratory of Special Elastomeric Composite Materials, Beijing Institute of Petrochemical Technology, Beijing 102617, China; [2] Beijing Institute of Technology, Beijing 100081, China

Abstract: To improve the corrosion resistance of Ti6Al4V alloys in acid solution, a W-Mo co-penetrated top layer was prepared by hollow-cathode glow discharge plasma technique below the β phase transition point. The surface morphology, chemical composition and crystal structure of the coatings were determined by scanning electron microscopy (SEM), energy-dispersive X-ray spectroscopy (EDS) and X-ray power diffraction (XRD), respectively. Results indicate that a dense co-penetrated layer is produced with maximum thickness of approximately 23 μm. The layer is composed of $AlMoTi_2$ and Ti_xW_{1-x} phases. The static corrosion test is conducted in acid (H_2SO_4 and HCl, separately) at room temperature (RT) by the electrochemical workstation. The results show that the W-Mo co-penetrated layer could achieve relatively stable corrosion potential in reducing acid and the I_{corr} of co-penetrated layers occupy merely 1/10 and 1/6 of that of Ti6Al4V substrates. In addition, there is barely any corroded product and crack on the corroded surface of co-penetrated layers, indicating no corroded shedding phenomenon occurs. So the corrosion resistance are obviously improved in the premise of keeping the basic properties of the substrate.

Key words: Ti6Al4V; W-Mo co-penetrated layer; glow discharge; corrosion resistance

Titanium and titanium alloys have been widely used due to their outstanding properties such as high specific strength, corrosion resistance and biocompatibility[1-3]. Essentially, strong acids are chemically aggressive to materials and plant in them. In addition, these materials are exposed to different corrosion tests depending on the utilizing environment and the nature of the material itself[4-6]. Titanium and titanium alloys matrix composites reinforced with high strength modified layers such as Mo-Cr, Ti-N, and Cu-Ti have attracted more and more attention in the past few decades[7-9]. Among them, the W-Mo co-penetrated layer produced by glow discharge plasma technique is one of the preferred representative[10].

In recent years, various ceramic coatings (e.g., TiC, TiO_2, TiN and TiB) have been synthesized to improve the surface properties of Ti alloys by chemical vapor deposition, magnetron sputtering, electron beam evaporation, or electrochemical deposition[11-14]. Liu et al.[15] investigated the corrosion and tribological behavior of chromium oxide coatings prepared by a duplex treatment of chromizing followed by plasma oxidizing. A significant decrease in average friction coefficient and an excellent corrosion resistance have been obtained. Fossati et al.[16,17] investigated the corrosion resistance of glow-discharge nitrided samples in acid solutions. It indicated that the glow-discharge nitrided samples possessed higher electrochemical inertia and lower corrosion currents than the untreated alloy after a period of immersion in high oxidizing acid solution. Rossi et al.[18] confirmed that the 750 °C nitrided samples have poorer behavior than those treated at 900 °C due to the limited thickness of the modified layer and the lower corrosion resistance of nitride ε formed in the nitrided layer.

However most of the studies focused on coatings

corrosion behaviors in 3.5 wt% NaCl solution[19-21]. Unfortunately, another equally important issue for structural applications of their corrosion behaviors in acid at RT, was often neglected. In the present work, a W-Mo co-penetrated layer was prepared on the Ti6Al4V substrate by hollow-cathode glow discharge plasma technique below the β phase transition point. The corrosion behaviors of the W-Mo alloying layer were investigated to make a comprehensive assessment and to support the application of this surface-alloying technology.

1   Experiment

The hollow-cathode plasma glow discharge system employed in this paper is schematically given in Fig.1. An inverted bucket surrounding the workload worked as anode. The multilayer covers stabilize the co-penetrated atmosphere and generate more W-Mo ions. As a result, even when the substrate temperature was below β phase transition point, the W-Mo ions could deposit and diffuse into the matrix. The source electrode, acicular source (made up of W-Mo alloy) and sample holder (made up of AISI 304 stainless steel), placed in the centre of the treatment chamber, worked as a cathode. Once heated to a given temperature, the surface activity of substrate electrode was enhanced due to the Ar+ bombardment. The ions and atoms deposited and diffused into the matrix; thus, an alloying layer was developed on the substrate.

The sputtering target was a slice cut from W-Mo alloy with a diameter of 20 mm. The substrates were commercially available Ti6Al4V with a three-dimensional size of 15 mm × 15 mm × 5 mm. Prior to deposition, the substrates were machined, ground, and polished in sequence, then ultrasonically cleaned in acetone and dried in air. Other parameters are: target/substrate distance (8 cm); base pressure (<1 Pa); working gas pressure (Argon, 99.99%, 30 Pa); sputtering voltage (750 V); substrate temperature (800 °C); and deposition time (6 h).

The cross-sectional morphology and elemental distribution were detected by the scanning electron microscope (SEM, SSX-550) and energy dispersive X-ray
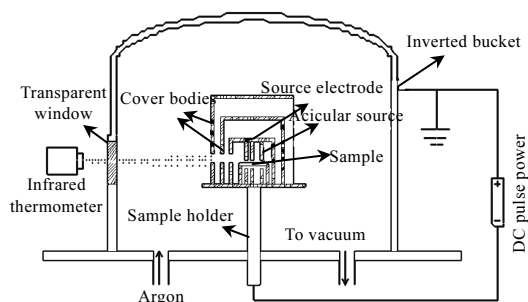
spectroscope (EDS) respectively. The crystal structure of the co-penetrated layer was measured by the X-ray diffractometer (XRD, Bruker D8-Focus) with Cu Kα radiation ($\lambda = 0.15406$ nm), generated at 40 kV voltage and 40 mA.

The corrosion behaviors were evaluated in sulfuric acids (H_2SO_4, 10 wt% and 40 wt%) and hydrochloric acid (HCl, 10 wt% and 20 wt%) solutions. All measurements were performed using an electrochemical workstation (CS360) at RT. The saturated calomel electrode (SCE) was used as a reference electrode and the counter electrode (CE) was a platinum plate. The coated and uncoated specimens were employed as working electrodes (WE), with a naked geometric area of 1 cm^2. Potentiodynamic tests were performed on specimens after 1 h of immersion to achieve a stable open circuit potential (OCP), with a scanning rate of 0.5 mV/s from -1000 mV vs. OCP to + 1000 mV vs. OCP. The surface morphology and phase composition after corrosion were analyzed by SEM and XRD. In addition, each test was repeated three times for all specimens.

2   Results

2.1   Morphology and elemental distributions

Fig.2 shows the XRD pattern of untreated and co-penetrated Ti6Al4V samples. The alloying layer mainly consists of AlMoTi$_2$ and Ti$_x$W$_{1-x}$ phases which are the thermodynamically stable phases. The result of cross-sectional scanning of the treated sample is demonstrated in Fig.3. It can be seen that the co-penetrated layer consists of two different layers, the outer one is a W-Mo deposited layer and the inner one is a diffused layer. The existence of the diffusion layer contributes a robust adhesion between the deposited layer and the matrix. The co-penetrated layer is continuous and compact, which exhibits higher chemical stability than Ti6Al4V substrate. Compared with double glow-discharge plasma surface alloying, there is no phase transition in the process[18].

Fig.4 shows the cross-sectional EDS line analysis of the co-penetrated layer. The white line in Fig.3 is the investigation

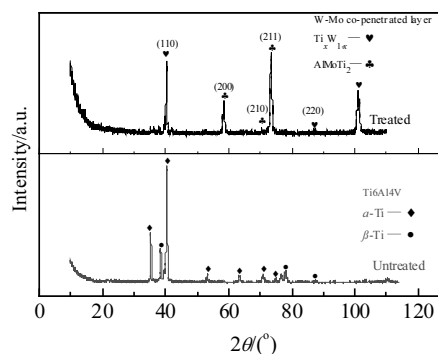Fig.1   Schematic diagram of the alloying system

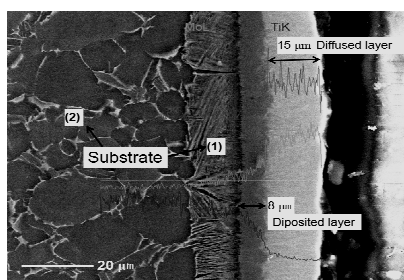Fig.2   XRD patterns of untreated and co-penetrated Ti6Al4V samples

Fig.3   SEM cross-sectional morphology of W-Mo co-penetrated layer

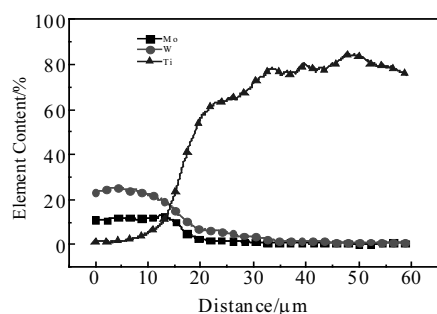Fig.4   Cross-sectional elemental distribution of the co-penetrated layer

Fig.5   Potentiodynamic polarization curves of specimens in 10 wt% (a) and 40 wt% (b) H_2SO_4 solutions

line of the composition distribution. The concentration of W and Mo decreases gradually and the maximum content of W approximates to 30 according to the results of EDS line analysis. In the diffusion layer, the proportion of other elements keeps constant comparing to that of the matrix. So the diffusion of Mo and W achieved may be along crystal defects[20], which strengthen the interface combination between the depositing layer and the matrix. Besides, the concentration of Ti element in the (1) area approximates to that in (2) area, and neither the W element nor the Mo element is detected in the (1) area. It indicates that grain refinement occurs during the treating process.

2.2   Electrochemical corrosion behaviors

Fig.5 illustrates the potentiodynamic polarization curves of the specimens in H_2SO_4 solutions (10 wt% and 40 wt%). Compared with the Ti6Al4V substrates, the OCP of the W-Mo co-penetrated layers increases by 110 and 50 mV, respectively. In the 10 wt% H_2SO_4 solution, for substrates, the passivation behaviors both occur at potential values of 320 mV (Ti6Al4V substrate) and –290 mV (W-Mo co-penetrated layer). In the 40 wt% H_2SO_4 solution, however, passivation is observed at –390 mV (Ti6Al4V substrate) and –310 mV (W-Mo layer). The discrepancy should be attributed to the presence alloying layer covering the entire surface, which will block the corrosive media diffusion to substrate and thus slows down the corrosion
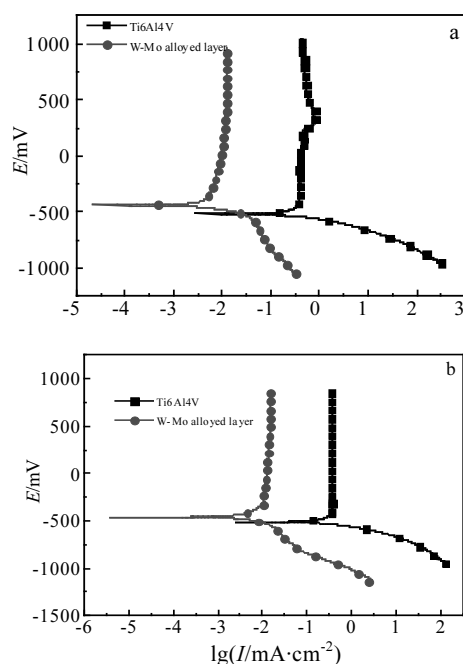
rate. Therefore galvanic corrosion may occur between the alloying layer and the substrate, in which the substrate is anodically corroded. The obvious positive shift of E_{corr} reveals the enhancement in corrosion resistance.

The OCP, passivation potential (E_{pass}), current density (I_{corr}) and annual corrosion rate (I_a) obtained in H_2SO_4 solutions are listed in Table 1. I_a of W-Mo co-penetrated layer are 4.47×10^{-3} and 6.34×10^{-2} mm/a, merely 1/15 and 1/13 of that of the substrate, respectively. In addition, I_{corr} of the substrate is almost ten times that of the W-Mo co-penetrated layer. It demonstrates that the corrosion resistance of the Ti6Al4V substrate is significantly improved by the surface alloying technique. It should be attributed to the diffused W and Mo elements, which reinforce the thermodynamic stability and finally improve the corrosion resistance of the Ti6Al4V substrate [7].

Fig.6 illustrates the potentiodynamic polarization curves

Table 1   Electrochemical corrosion results of specimens in H_2SO_4 solution

Specimen	H_2SO_4/wt%	OCP/mV	E_{pass}/mV	I_{corr}/mA·cm^{-2}	I_a/mm·a^{-1}
TC4	10	−530	−290	1.04×10^{-1}	6.89×10^{-2}
Alloying layer		−420	−320	1.25×10^{-2}	4.47×10^{-3}
TC4	40	−510	−390	9.98×10^{-1}	8.42×10^{-1}
Alloying layer		−460	−310	1.89×10^{-1}	6.34×10^{-2}

of the specimens in 10 wt% and 20 wt% HCl solutions. It can be observed that the E_{corr} values for W-Mo co-penetrated layer toward the positive direction have increased by 70 mV and 56 mV comparing to Ti6Al4V substrates, respectively. However, no passivation behavior occurs for both the substrate and the W-Mo layer in HCl solutions, which differs from those in the H_2SO_4 solutions.

Table 2 shows OCP, E_{pass}, I_{corr} and I_a obtained using both cathodic and anodic branches of the Tafel curves. As shown in Table 2, I_a of W-Mo co-penetrated layers are 4.37×10^{-3} and 5.48×10^{-3} mm/a, only 1/5 and 1/7 of that of the TC4 substrates in 10 and 40 wt% HCl solutions, respectively. Moreover, I_{corr} of the substrate is almost six times that of the W-Mo co-penetrated layer in HCl solution.

3 Discussion

The results listed in the previous sections clearly indicate that the W-Mo co-penetrated layer significantly influences the corrosion resistance properties of Ti6Al4V alloy.
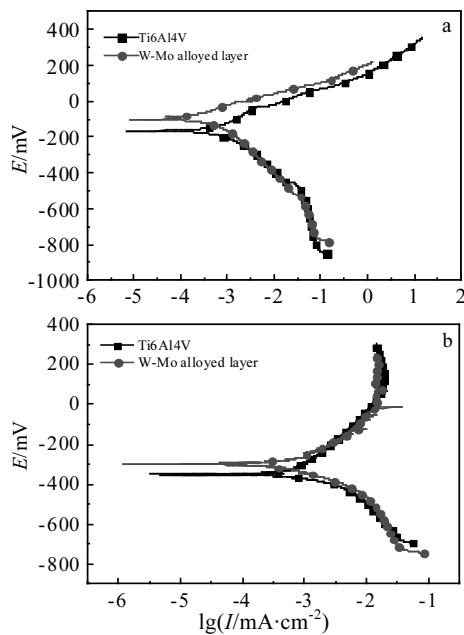

Fig.6　Potentiodynamic polarization curves of specimens in 10 wt% (a) and 20 wt% (b) HCl solution

Table 2 Electrochemical corrosion results of specimens in HCl solutions

Specimen	HCl/ wt%	OCP/ mV	E_{pass}/ $\times10^{-2}$mV	I_{corr}/ mA·cm^{-2}	I_a/ mm·a^{-1}
TC4	10	−100	5.40	1.94×10^{-2}	1.94×10^{-2}
Alloying layer		−170	1.22	4.37×10^{-3}	4.37×10^{-3}
TC4	20	−300	9.84	3.53×10^{-2}	3.53×10^{-2}
Alloying layer		−356	1.53	5.48×10^{-3}	5.48×10^{-3}

Fig.7 shows the corroded surface morphologies of Ti6Al4V substrates after immersed in H_2SO_4 (40 wt%) and HCl (20 wt%) for 15 d. A lot of pits with the maximum diameter of 25 μm and cracks are observed on the corroded surface. From the further enlarged observation (insert pictures), the corroded products tend to be loose and drop off the specimens as a result of the corrosion pits. As reported, the corrosion damaging is quite generalized and uniform inside the crevices suggesting an active corrosion mechanism[16], probably due to the decrease of the local pH values inside the crevices.

Fig.8 and Fig.9 illustrate the XRD patterns of the corroded surface, where $TiH_{1.5}$, TiH, TiO and $TiO_{1.04}$ peaks are detected. However, no TiO_2 phases are detected after immersed in the reducing acid solution.

The dissolution reaction of titanium oxide:

$$TiO_x + 2xH^+ = Ti^{2x+} + xH_2O \tag{1}$$

The overall reaction of titanium in strong reducing acid:

$$2Ti + 6H^+ = 2Ti^{3+} + 3H_2 \tag{2}$$
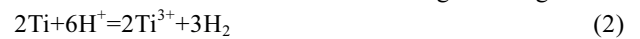
Fig.10 shows the SEM morphologies of W-Mo co-penetrated layer after immersed in 40% H_2SO_4 and 20% HCl for 15 d. It should be noted that the surface of W-Mo co-penetrated layer appears to be almost uninfluenced and barely a localized corrosion is visible in very few points (Fig.10a). There is barely any corroded products on the corroded surface, indicating no corroded shedding phenomenon. Furthermore, SEM analysis has shown that the localized corrosion can be attributed to the nucleation of few small pits. In the case of samples tested in 20% HCl solution even if no appreciable crevice attack is present very little amount of corroded products are observed, suggesting
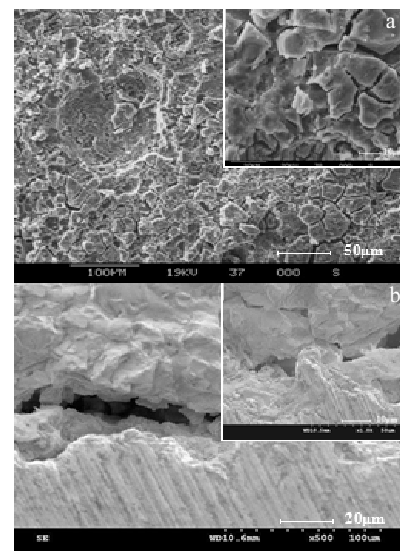

Fig.7　Corroded surface morphologies of Ti6Al4V substrates after immersed in 40% H_2SO_4 (a) and 20% HCl (b) solutions for 15 d (insets show the partial enlargements of the overall views)
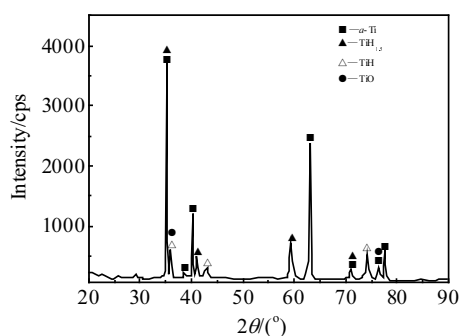
Fig.8   XRD pattern of Ti6Al4V substrates after immersed in 40% H_2SO_4 solution
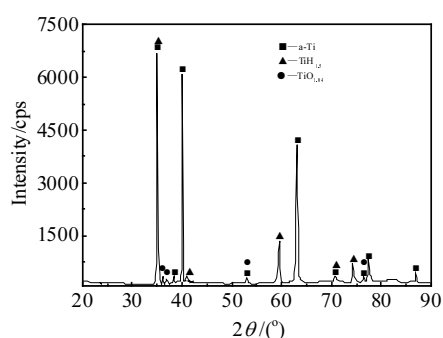

Fig.9   XRD pattern of Ti6Al4V substrates after immersed in 20% HCl solution
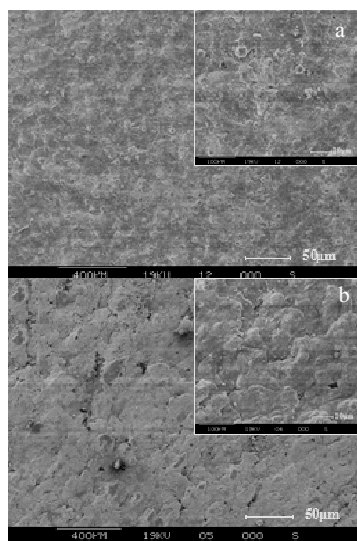

Fig.10   Corroded surface morphologies of W-Mo co-penetrated layer in 40% H_2SO_4 (a) and 20% HCl (b) (insets show the partial enlargements of the overall views)

the presence of very light corrosion process, probably occurring at the grain boundary[22].

The improvement in corrosion performance could be attributed to two major factors. Firstly, it is well established that continuous and compact structures lead to the improvement of corrosion resistance, due to the formation of a protective W-Mo co-penetrated layer. Since the alloying layer formed on the substrate is allowed to be cool in the furnace rather than in air, it possesses a lower porosity. It is believed that the corrosion resistance is improved due to the coverage of its surface by W-Mo co-penetrated layer, which serves as an effective barrier layer, physically separated it from the acid medium. Secondly, the presence of $AlMoTi_2$ and Ti_xW_{1-x} phases which reinforce the thermodynamic stability significantly reduces the rate of corrosion. And in addition, it can also be deduced and inferred that an increase of W-Mo elements in the content leads to the improvement in the corrosion resistance of Ti6Al4V[23].

4   Conclusions

1) Using a hollow-cathode glow discharge plasma technique, W-Mo co-penetrated layer is produced onto Ti6Al4V substrate below the β phase transition point. The W-Mo co-penetrated layer could achieve higher corrosive polarization resistance and relatively stable corrosion potential in acid (H_2SO_4 and HCl).

2) The I_{corr} of W-Mo co-penetrated layers occupy merely 1/10 and 1/6 of that of Ti6Al4V substrates at room temperature. Therefore, hollow-cathode glow discharge co-penetrated treatment, performed below the β phase transition point, is an effective technique to largely increase the corrosion resistance in reducing acid of Ti6Al4V substrate.

References

1   Ji Shouchang, Li Zhengxian, Do Jihong *et al. Rare Metal Materials and Engineering*[J], 2010, 39(12): 2152

2   Hua Yunfeng, Li Zhengxian, Yang Hao *et al. Rare Metal Materials and Engineering*[J], 2012, 41(12): 2131

3   Li Zhengxian, Du Jihong, Zhou Hui *et al. Rare Metal Materials and Engineering*[J], 2004, 33(11): 1174

4   Meng W J, Zhang X D, Shi B *et al. Mater Res*[J], 2002, 17(10): 2628 (in Chinese)

5   Yang S M, Chang Y Y, Wang D Y *et al. J Alloy Compd*[J], 2007, 440(1): 375

6   Chen F, Li C M, Lv F X. *Rare Metals*[J], 2007, 26(2): 142

7   Ren B L, Miao Q, Liang W P *et al. Surface and Coatings Technology*[J], 2013, 228(S1): 206

8   Jin X M, Gao L Z, Liu E Q *et al. Science Direct*[J], 2015, 6(4): 1751

9   Yu X M, Tan L L, Yang H Z *et al. J Alloy Compd*[J], 2015, 646(4): 925

10   F Borgioli, Galvanetto E, Galliano F P *et al. Surface and Coatings Technology*[J], 2014, 141(1): 103

11   Liu C, Leyland A, Matthews A. *Surface and Coatings Technology*[J], 2001, 141(2-3): 164

12 Paulitsch J, Mayrhofer P H, Münz W D *et al. Thin Solid Films*[J], 2008, 517(3): 1239

13 Pandiyaraj K N, Selvarajan V, Rhee Y H *et al. Colloids & Surfaces B Biointerfaces*[J], 2010, 79(1): 53

14 Wron Ski Z, Filik J. *Vacuum*[J], 2014, 83(S1): 77

15 Liu H B, Tao J, Xu J *et al. Surface & Coating Technology*[J], 2009, 204(1-2): 28

16 Fossati A, Borgioli F, Galvanetto E *et al. Corrosion Science*[J], 2004, 46(4): 917

17 Galvanetto E, Galliano F P, Fossati A *et al. Corrosion Science*[J], 2002, 44(7): 1593

18 Rossi S, Fedrizzi L, Bacci T *et al. Corrosion Science*[J], 2003, 45(3): 511

19 Ma G J, Lin S L, Gong X *et al. Vacuum*[J], 2013, 89: 244

20 Ren B L, Qiang M, Liang W P e*t al. Surface and Coatings Technology*[J], 2013, 228(S1): 206

21 Mutiu F, Erinosho, Esther T *et al. Materials Today*[J], 2015, 2(4-5): 1166

22 Liu H X, Xu Q, Zhang X W *et al. Thin Solid Films*[J], 2012, 521: 89

23 Wang Q, Zhang P Z, Wei D B *et al. Materials & Design*[J], 2013, 49(1): 1042

等离子体辉光放电制备 W-Mo 共渗层在酸性溶液中耐蚀性研究

陈 飞 [1]，张玉林 [1]，刘伟光 [2]，冯文然 [1]，杨英歌 [1]

(1. 北京石油化工学院 特种弹性体复合材料北京市重点实验室，北京 102617)

(2. 北京理工大学，北京 100081)

摘　要：在 β 相变点以下，通过空心阴极等离子体辉光放电技术，在 Ti6Al4V 合金表面形成 W-Mo 共渗层来提高钛合金基体在酸性溶液中的耐蚀性。分别利用扫描电子显微镜、能谱仪和 X 射线衍射仪对试样的表面形貌、成分分布和相组成进行分析。结果显示在 Ti6Al4V 合金表面形成一层约 23 μm 厚，由 $AlMoTi_2$ 和 Ti_xW_{1-x} 物相组成的共渗层。利用电化学工作站，在常温静态条件下，对试样在酸性溶液中进行耐蚀性研究。结果表明，经过共渗处理的试样在酸性溶液中，能保持稳定的腐蚀电位并且其腐蚀电流密度仅为原始试样的 1/10 和 1/6。此外，相较于钛合金基体，处理后的试样表面没有发现腐蚀产物和裂纹，表明没有腐蚀脱落现象发生。因此，在保证基体基本性能的前提下，钛合金试样的耐蚀性能明显提高。

关键词：Ti6Al4V；W-Mo 共渗；辉光放电；耐蚀性

作者简介：　陈　飞，男，1971 年生，博士，教授，北京石油化工学院材料科学与工程学院，北京 102617，电话：010-81292097，E-mail: chenfei@bipt.edu.cn